

Physics of compact stars in NEUMATT (...and Ferrara)

Giuseppe Pagliara

Dipartimento di Fisica e Scienze della Terra, Università
di Ferrara and INFN



TNPI2017 3-5 October 2017

NEUMATT

(NEUtron star MATTer)

NEUMATT (previous name
NUMAT): ~16 FTE

national coordinator

Alessandro Drago

Nodes:

- Sez. Catania
- LNS
- LNGS
- Sez. Pisa
- Sez. Ferrara
- (+Politecnico Torino)
- Sez. Milano



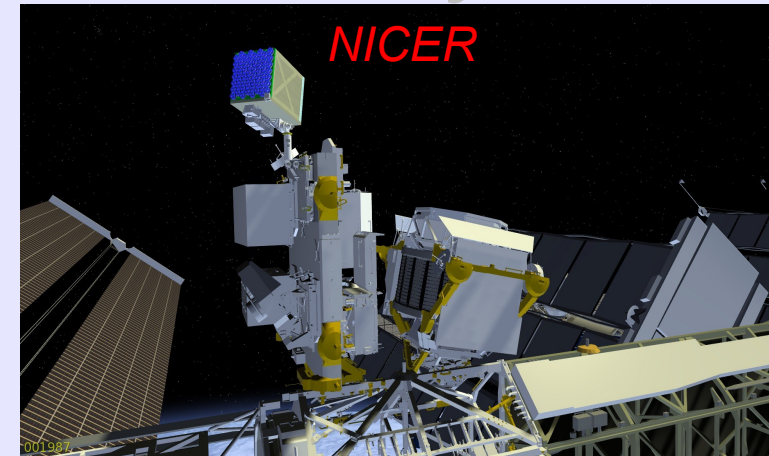
Strong connection with the IS:
MANYBODY, SIM, TEONGRAV

Goal of the IS

- Investigate the properties of strongly interacting matter at high densities (and small temperatures) through the study of compact stars
- Provide realistic calculations of equations of state and transport properties for baryonic matter (nucleons, hyperons, deltas) and quark matter (pure phases or mixed phases).
- Use of them for: structure of compact stars, cooling and flares, glitches, explosive phenomena (supernovae and gamma ray bursts) and merger of compact stars (gravitational waves).

Why is Neumatt very interesting: Upcoming measurements: X-rays

NICER (Neutron star Interior Composition Explorer) on the ISS, is collecting data since June 2017.



Temporal pulse profile of the hot spot will allow to measure the radius within 5% of error. Radii strongly depend on the adopted equation of state (see in the following). Possibility to test the models produced by Neumatt.

The closest and brightest millisecond pulsar

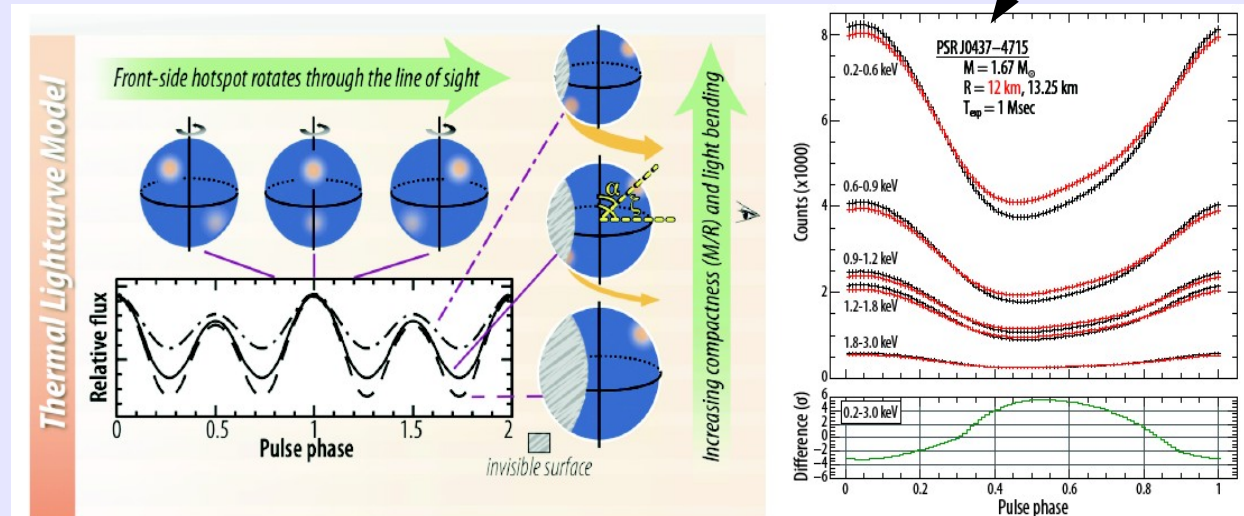
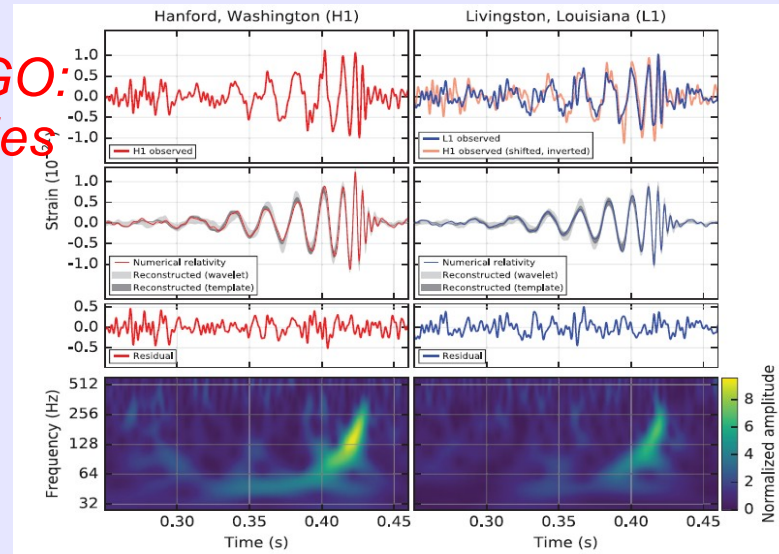


Figure 4. (Left) A distant observer sees X-ray intensity grow and fall as hot-spots on a neutron star surface spin through the line of sight. The far-side spot becomes more visible for smaller stars through gravitational light-bending, which depends on M/R ; thus, depth of modulation constrains compactness. (Right) Two sets of simulated NICER lightcurves, for stellar radii differing by $\pm 5\%$, show measurable differences in several energy bands for a 1 Msec exposure: 4- 6σ differences per phase bin pinpoint the star's radius.

Upcoming measurements: gravitational waves

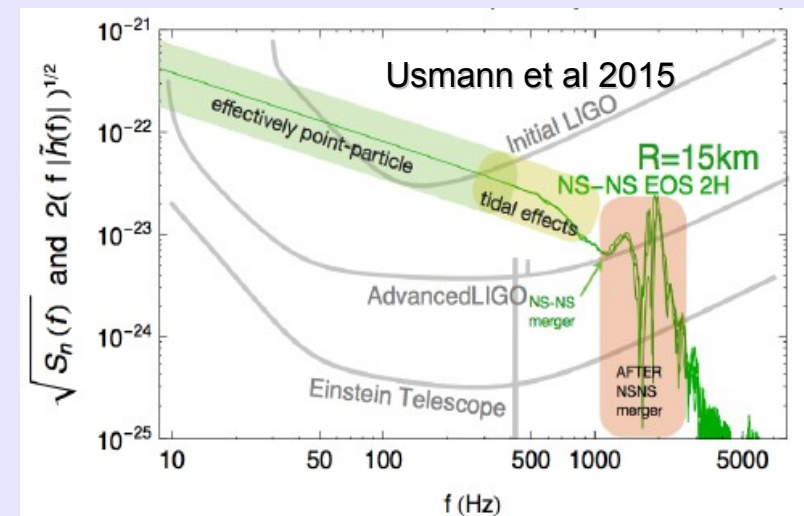
First direct detection by LIGO: September 2015: black-holes merger (PRL 116(2016)061102).
 3 M_{sun} of energy into Gws.
 First VIRGO detection announced 27/09/2017



LIGO & VIRGO



Also NS-NS merger will be soon (if not already ;-)) detectable: dimmer signal but higher event rate. Moreover: also the postmerger signal could be detected. GW spectrum strongly dependent on the compactness of the NS and thus on the equation of state. Stiff: low frequencies, soft: high frequencies. Event rate (very uncertain): 1-10 events per year. Test Neumatt predictions for the GWs signal.



Upcoming measurements: radio

Square kilometer array.

Construction planned in 2018, data taking from 2020.

It will allow to discover 10^4 more pulsars, among which 100 in binaries \rightarrow 100 new mass measurements (masses higher than $2M_{\text{sun}}$?)

Possible to extract the momentum of inertia which together with a mass measurement will strongly constrain the equation of state. Test Neumatt calculations on rotating compact stars.



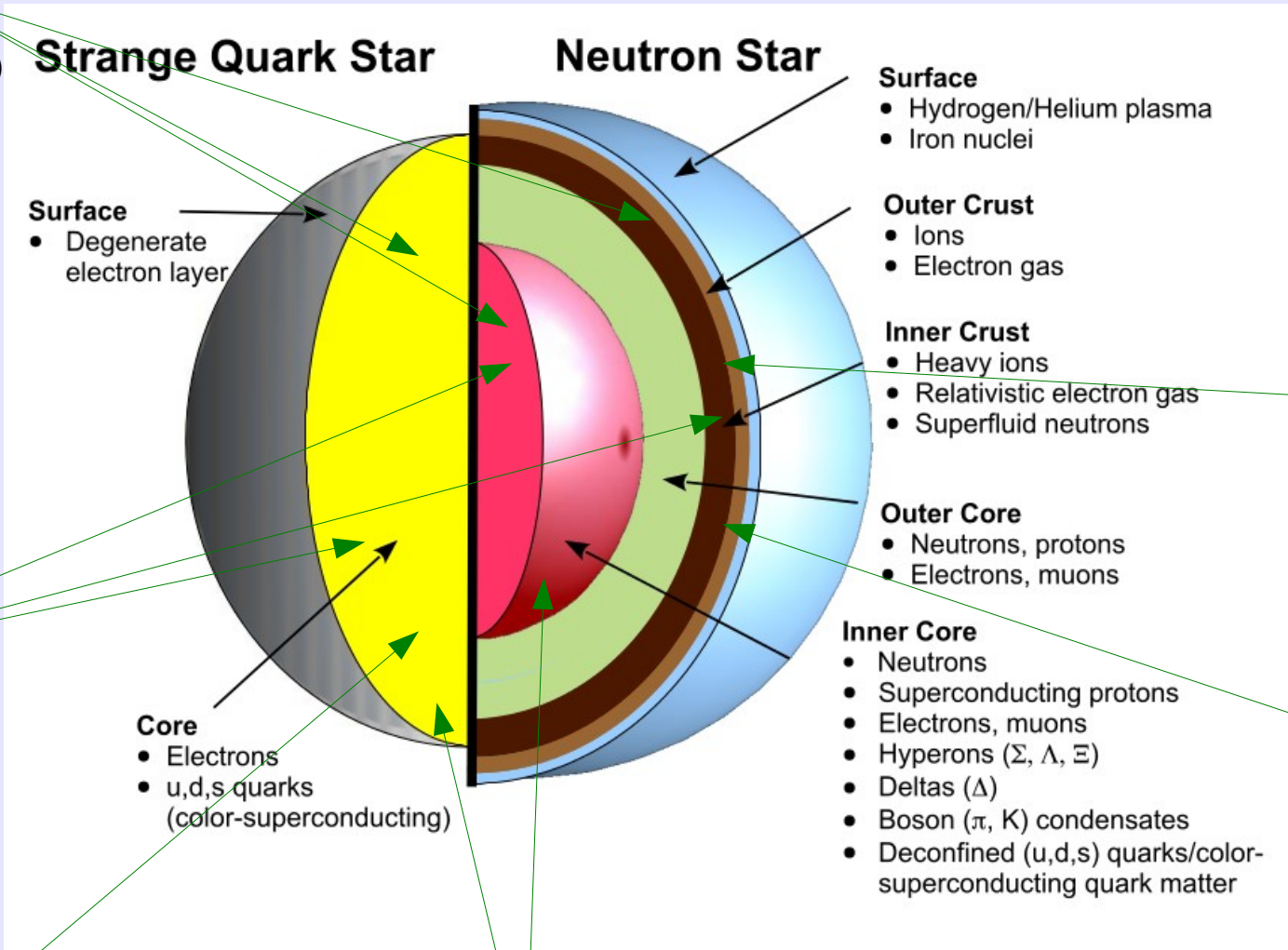
Gamma-ray-bursts events: SWIFT, FERMI in hard X-ray/soft gamma. Some GRBs may be generated by compact stars (magnetars). Some (indirect) info on the properties of matter already proposed (Gao et al. PRD 2016). Test Neumatt modeling of explosive phenomena.



Theoretical calculations of Neumatt:

CT

(see talk of I. Vidana)



PI

(see talk of D. Logoteta)

MI

(see talk of M. Antonelli)

LNS

LNGS

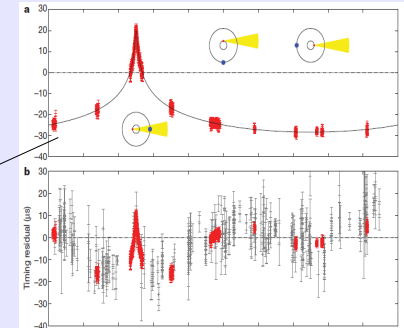
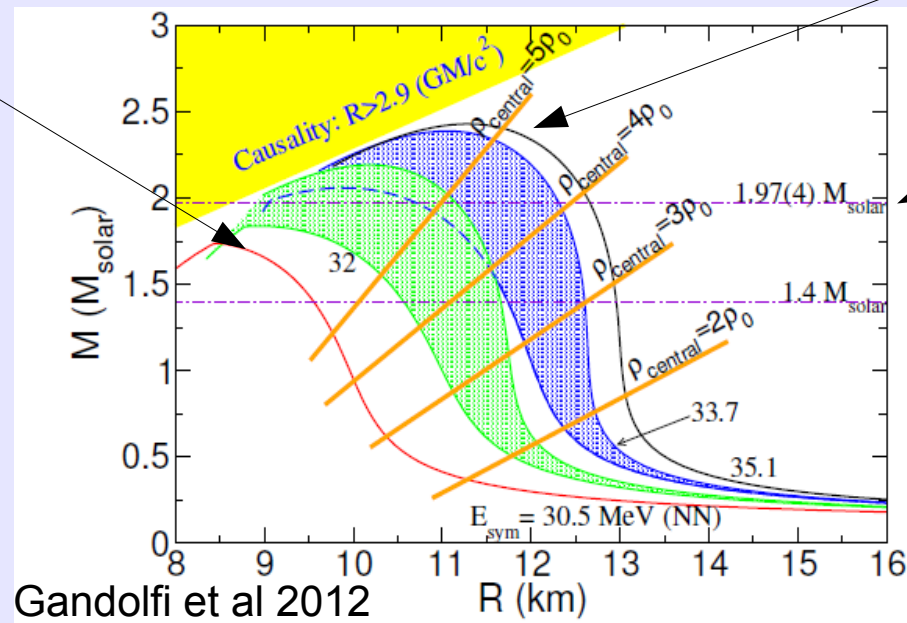
(see talk of M. Mannarelli)

FE

Soft and stiff EoSs

Soft: small maximum mass – compact configurations, large central densities, large central baryon chemical potential (which could reach 1.5 GeV, hyperons and deltas?)

Stiff: high maximum mass – less compact configurations, small central densities, small central baryon chemical potential



Strongest and reliable constraint from Shapiro delay: maximum mass of at least $2M_{\text{sun}}$

Having precise radii measurements would be very constraining, but...

Example of two radii measurements

THE NEAREST MILLISECOND PULSAR REVISITED WITH *XMM-NEWTON*: IMPROVED MASS–RADIUS CONSTRAINTS FOR PSR J0437–4715

SLAVKO BOGDANOV

Columbia Astrophysics Laboratory, Columbia University, 550 West 120th Street, New York, NY 10027, USA; slavko@astro.columbia.edu and

Department of Physics, McGill University, 3600 University Street, Montreal, QC H3A 2T8, Canada

Received 2012 July 17; accepted 2012 November 17; published 2012 December 19

ABSTRACT

I present an analysis of the deepest X-ray exposure of a radio millisecond pulsar (MSP) to date, an X-ray *Mirror-Newton* European Photon Imaging Camera spectroscopic and timing observation of the nearest known MSP, PSR J0437–4715. The timing data clearly reveal a secondary broad X-ray pulse offset from the main pulse by ~ 0.55 in rotational phase. In the context of a model of surface thermal emission from the hot polar caps of the neutron star, this can be plausibly explained by a magnetic dipole field that is significantly displaced from the stellar center. Such an offset, if commonplace in MSPs, has important implications for studies of the pulsar population, high energy pulsed emission, and the pulsar contribution to cosmic-ray positrons. The continuum emission shows evidence for at least three thermal components, with the hottest radiation most likely originating from the hot magnetic polar caps and the cooler emission from the bulk of the surface. I present pulse phase-resolved X-ray spectroscopy of PSR J0437–4715, which for the first time properly accounts for the system geometry of a radio pulsar. Such an approach is essential for unbiased measurements of the temperatures and emission areas of polar cap radiation from pulsars. Detailed modeling of the thermal pulses, including relativistic and atmospheric effects, provides a constraint on the redshift-corrected neutron star radius of $R > 11.1$ km (at 3σ conf.) for the current radio timing mass measurement of $1.76 M_{\odot}$. This limit favors “stiff” equations of state.

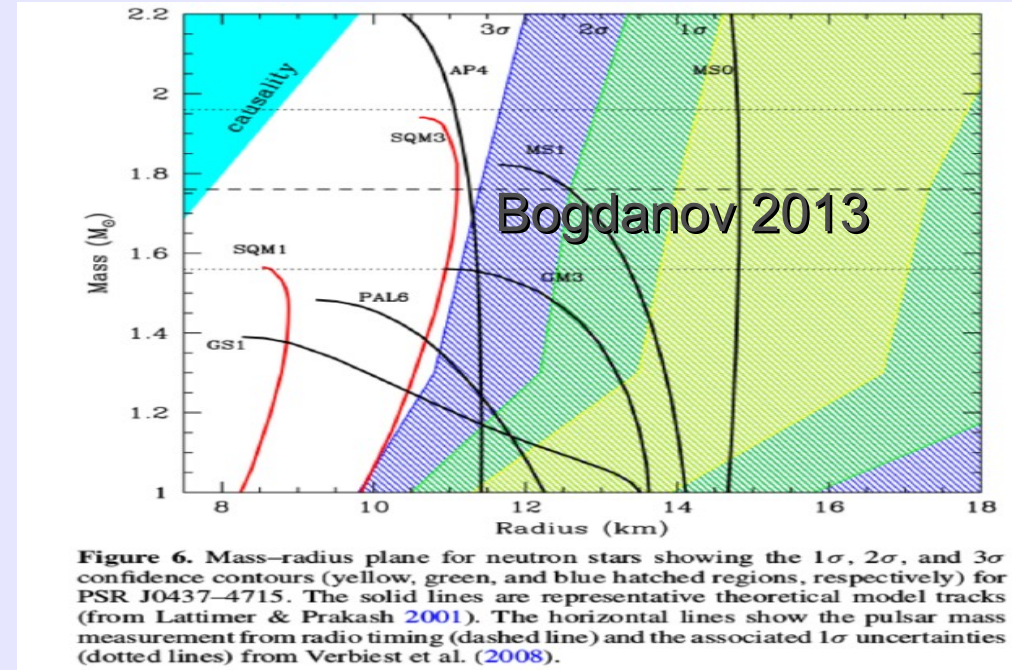


Figure 6. Mass–radius plane for neutron stars showing the 1σ , 2σ , and 3σ confidence contours (yellow, green, and blue hatched regions, respectively) for PSR J0437–4715. The solid lines are representative theoretical model tracks (from Lattimer & Prakash 2001). The horizontal lines show the pulsar mass measurement from radio timing (dashed line) and the associated 1σ uncertainties (dotted lines) from Verbiest et al. (2008).

NEUTRON STAR MASS–RADIUS CONSTRAINTS OF THE QUIESCENT LOW-MASS X-RAY BINARIES X7 AND X5 IN THE GLOBULAR CLUSTER 47 TUC

SLAVKO BOGDANOV¹, CRAIG O. HEINKE², FERYAL ÖZEL³, AND TOLGA GÜVER⁴

¹ Columbia Astrophysics Laboratory, Columbia University, 550 West 120th Street, New York, NY 10027, USA

² Department of Physics, University of Alberta, CCIS 4-183, Edmonton AB T6G 2E1, Canada

³ Department of Astronomy, University of Arizona, 933 North Cherry Avenue, Tucson, AZ 85721, USA

⁴ Istanbul University, Science Faculty, Department of Astronomy and Space Sciences, Beyazıt, 34119, Istanbul, Turkey

Received 2016 March 4; revised 2016 August 9; accepted 2016 August 18; published 2016 November 7

ABSTRACT

We present *Chandra*/ACIS-S subarray observations of the quiescent neutron star (NS) low-mass X-ray binaries X7 and X5 in the globular cluster 47 Tuc. The large reduction in photon pile-up compared to previous deep exposures enables a substantial improvement in the spectroscopic determination of the NS radius and mass of these NSs. Modeling the thermal emission from the NS surface with a non-magnetized hydrogen atmosphere and accounting for numerous sources of uncertainties, we obtain for the NS in X7 a radius of $R = 11.1^{+0.8}_{-0.7}$ km for an assumed stellar mass of $M = 1.4 M_{\odot}$ (68% confidence level). We argue, based on astrophysical grounds, that the presence of a He atmosphere is unlikely for this source. Due to the excision of data affected by eclipses and variable absorption, the quiescent low-mass X-ray binary X5 provides less stringent constraints, leading to a radius of $R = 9.6^{+0.9}_{-1.1}$ km, assuming a hydrogen atmosphere and a mass of $M = 1.4 M_{\odot}$. When combined with all existing spectroscopic radius measurements from other quiescent low-mass X-ray binaries and Type I X-ray bursts, these measurements strongly favor radii in the 9.9–11.2 km range for a $\sim 1.5 M_{\odot}$ NS and point to a dense matter equation of state that is somewhat softer than the nucleonic ones that are consistent with laboratory experiments at low densities.

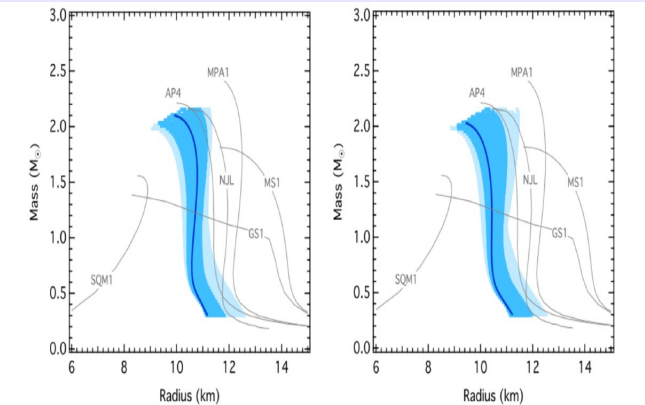


Figure 10. Mass–radius relation (solid blue curve) corresponding to the most likely triple of pressures that agrees with the current neutron star data. These include the X5 and X7 radius measurements shown in this work, as well the neutron star radii measurements for the 12 neutron stars included in Özel et al. (2016), the low-energy nucleon–nucleon scattering data, and the requirement that the EoS allow for a $M > 1.97 M_{\odot}$ neutron star. The ranges of mass–radius relations corresponding to the regions of the P_1, P_2, P_3 parameter space in which the likelihood is within $e^{-1/2}$ and e^{-1} of its highest value are shown in dark and light blue bands, respectively. The results for both flat priors in P_1, P_2 , and P_3 (top panel) and for flat priors the logarithms of these pressures (bottom panel) are shown.

Bogdanov et al 2016

Different stellar objects, different techniques... still, some indication of large stars (>12 km) and small stars (<11 km)

Symmetry energy

Recent results from ASY-EOS:
interpreting the data with URQMD

$$E_{\text{sym}} = E_{\text{sym}}^{\text{pot}} + E_{\text{sym}}^{\text{kin}} = 22 \text{ MeV}(\rho/\rho_0)^\gamma + 12 \text{ MeV}(\rho/\rho_0)^{2/3}$$

Extracted value of $L=72 \pm 13$ MeV. It determines the radius of the $M=1.4M_{\text{sun}}$ star (Lattimer&Lim 2013).

$$R_{1.4} \simeq 8.702 + 0.070L \text{ km}$$

Correlation (in RMF models) between L and the threshold for the appearance of deltas.

Russotto et al 2016 (CT-LNS)

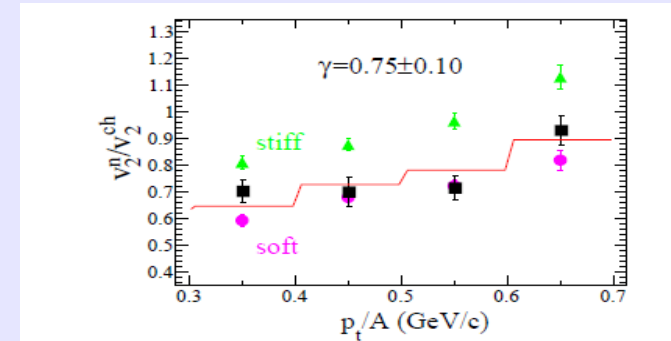
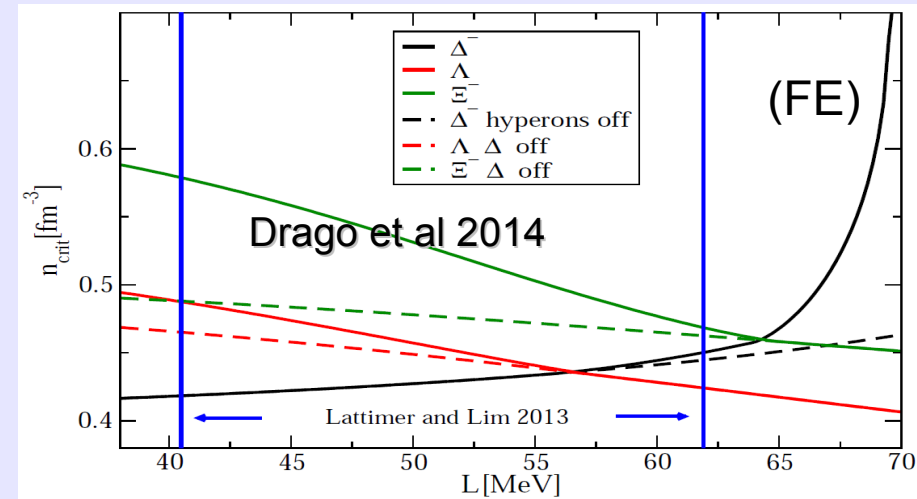


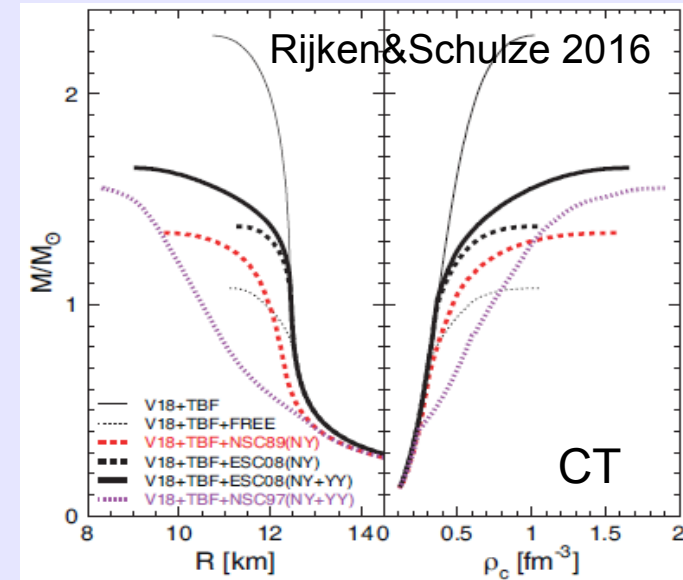
FIG. 14: Elliptic flow ratio of neutrons over all charged particles for central ($b < 7.5$ fm) collisions of $^{197}\text{Au}+^{197}\text{Au}$ at 400 MeV/nucleon as a function of the transverse momentum per nucleon p_t/A , evaluated with a fraction of 80% for the second step of timing corrections (see Sec. IV A). The black squares represent the experimental data; the green triangles and purple circles represent the UrQMD predictions for stiff ($\gamma = 1.5$) and soft ($\gamma = 0.5$) power-law exponents of the potential term, respectively. The solid line is the result of a linear interpolation between the predictions, weighted according to the experimental errors of the included four bins in p_t/A and leading to the indicated $\gamma = 0.75 \pm 0.10$.



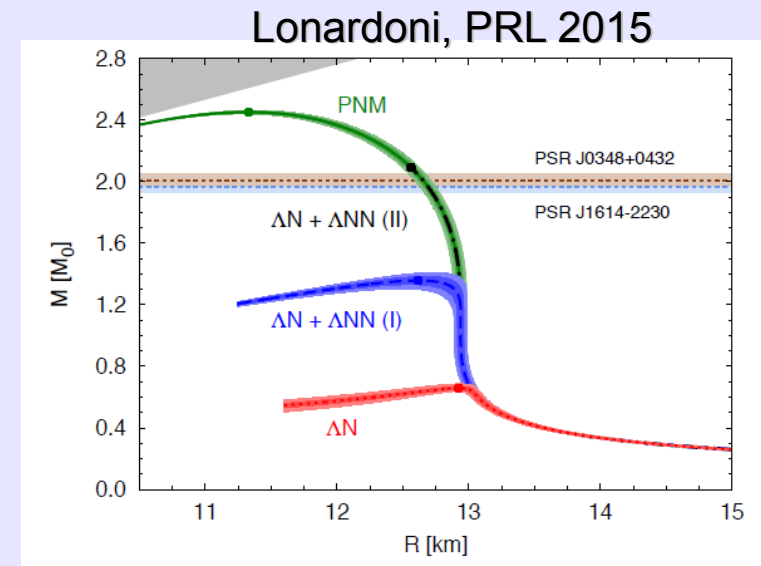
Hyperonic matter

Hyperon puzzle: hyperons must be included in the equation of state ...but many (microscopic) calculations (e.g. BHF in CT and PI) have proven that they soften the equation of state too much. Some recent results: not possible to reach $2M_{\text{sun}}$ but (at least) $1.6M_{\text{sun}}$.

(See also for CT BHF: Baldo, Eur.Phys.J. A(2016), Baldo et al PRC2017)



One possible solution: strong Λ - Λ repulsion, late appearance of hyperons, the $2M_{\text{sun}}$ stars have central densities below the threshold.
(See talk of Pederiva)



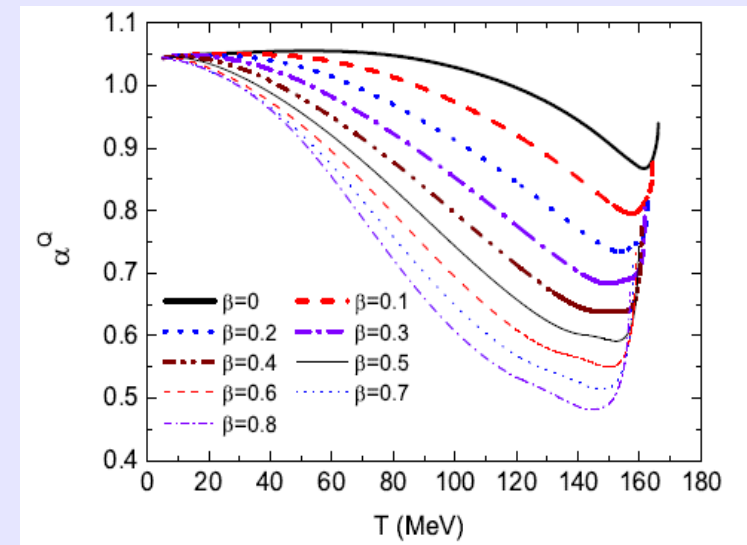
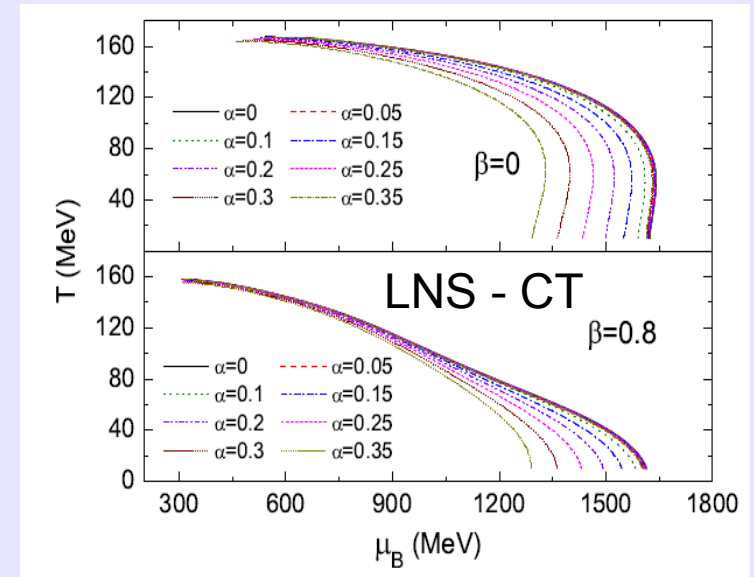
Dense and hot quark matter

Phase diagram within an improved Polyakov loop potential μ PNJL (with explicit dependence on the chemical potential, more suitable for low energy HIC and compact stars physics (SN & protoneutron stars)):

$$T_0(N_f, \mu) = T_\tau e^{-1/(\alpha_0 b(N_f, \mu))}$$

$$b(N_f, \mu) = \frac{11N_c - 2N_f}{6\pi} - \beta \frac{16N_f}{\pi} \frac{\mu^2}{T_\tau^2}$$

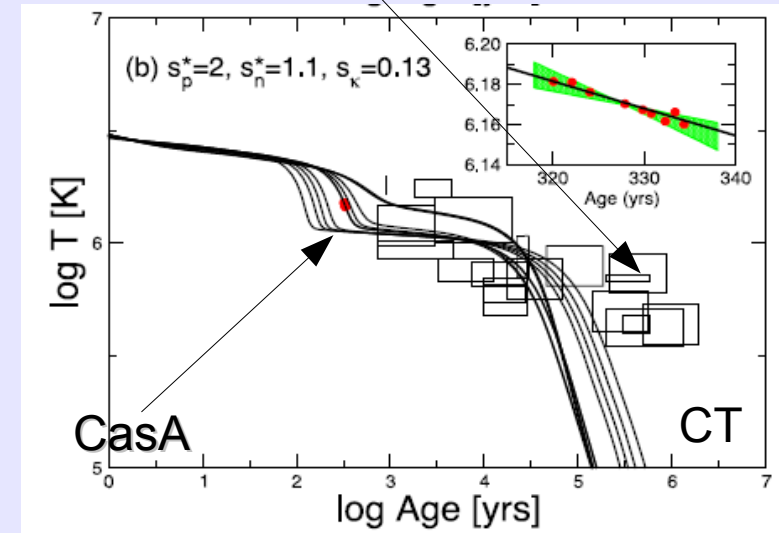
The beginning of the quark-hadron mixed phase is characterized by a large isospin asymmetry of the quark phase (smaller than in the normal PNJL though). Isospin distillation: expected enhancement of the π^-/π^+ at the onset of the phase transition. Stronger dependence on T wtr to the PNJL. Shao et al PRD2016



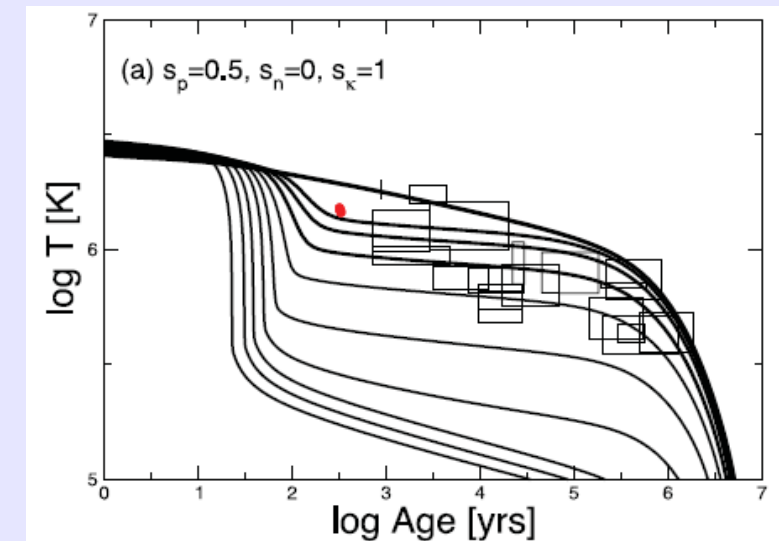
Cooling of neutron stars

Some data indicate slow cooling

The rapid cooling of CasA (observations over 15 years), challenges the theoretical modeling. Need of fine tuning on the proton and neutron gaps. Difficulties in explaining slow coolers.



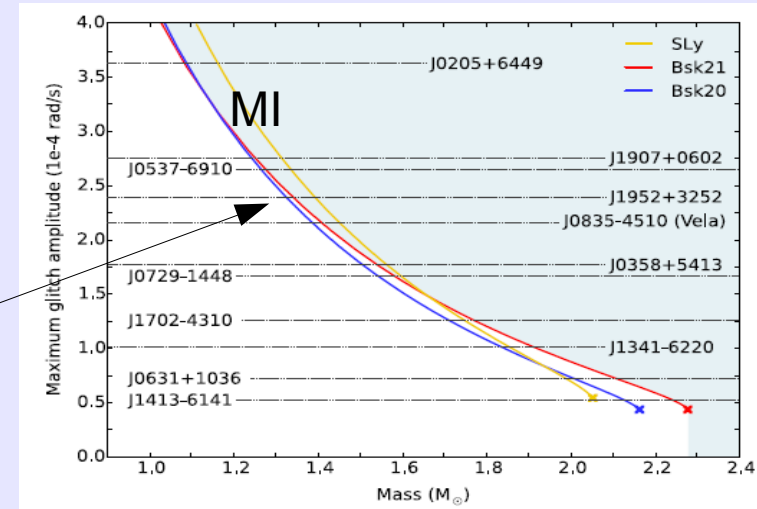
Equation of state and superfluid gap calculated consistently within the same model (BHF calculations). The fast cooling could also be due to DirectUrca processes (data reanalysis: no clear evidence of fast cooling of CasA)



Low density: crusts, glitches

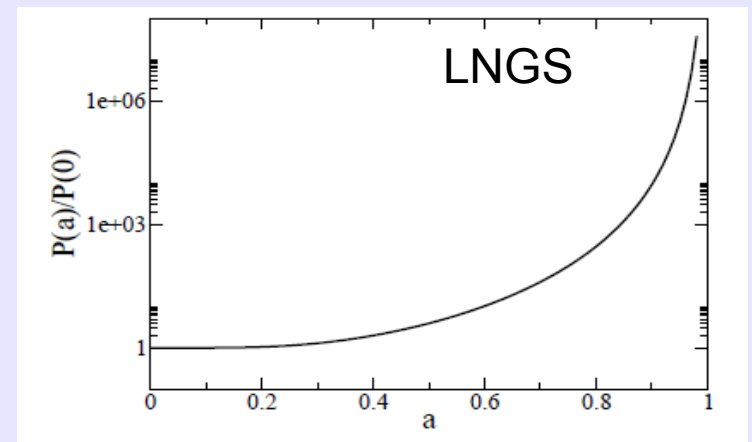
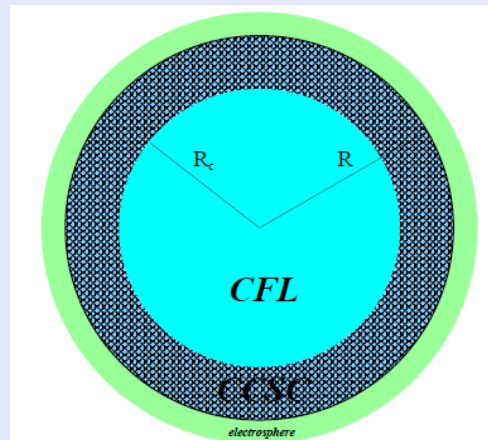
Inverse correlation between mass and maximum glitch amplitude: a new way to constrain neutron star masses

(Pizzochero et al Nat.Astron. 2016). New and stronger glitches from the same pulsar could eventually decrease the estimate of the mass which can be thus considered as an upper limit. (See talk of M.Antonelli)



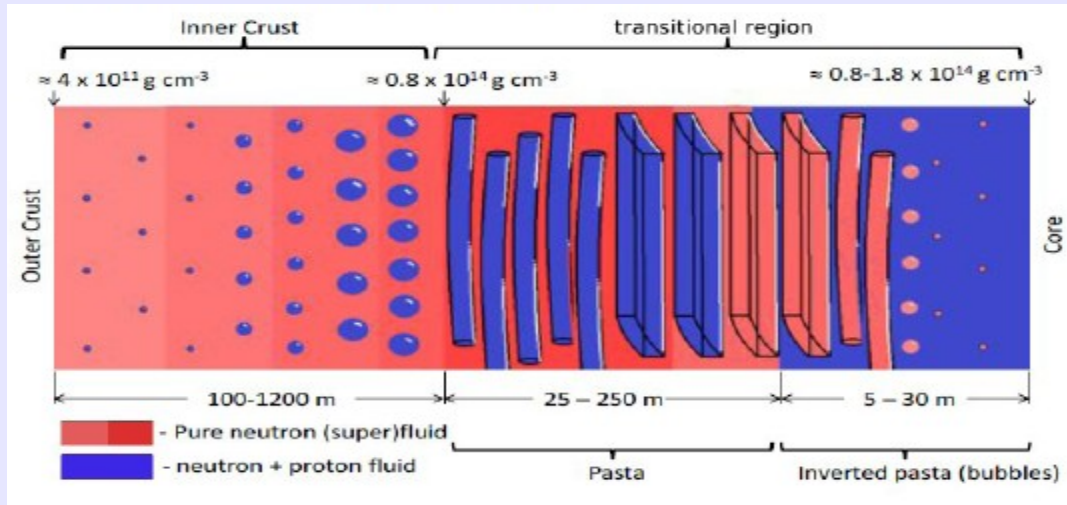
Power emitted of the order of 10^{45} erg/sec (for a thin crust), radio bursts of less than 1s. FRB??

Bare strange stars with crust made of crystalline color superconducting phase (LNGS): this phase has a very high rigidity. Excitations of torsional modes and strong EM emission due to the charged surface of bare strange stars. (Mannarelli et al PRD 2014)



ν -N scattering in protoneutron stars

(from M. Colonna)



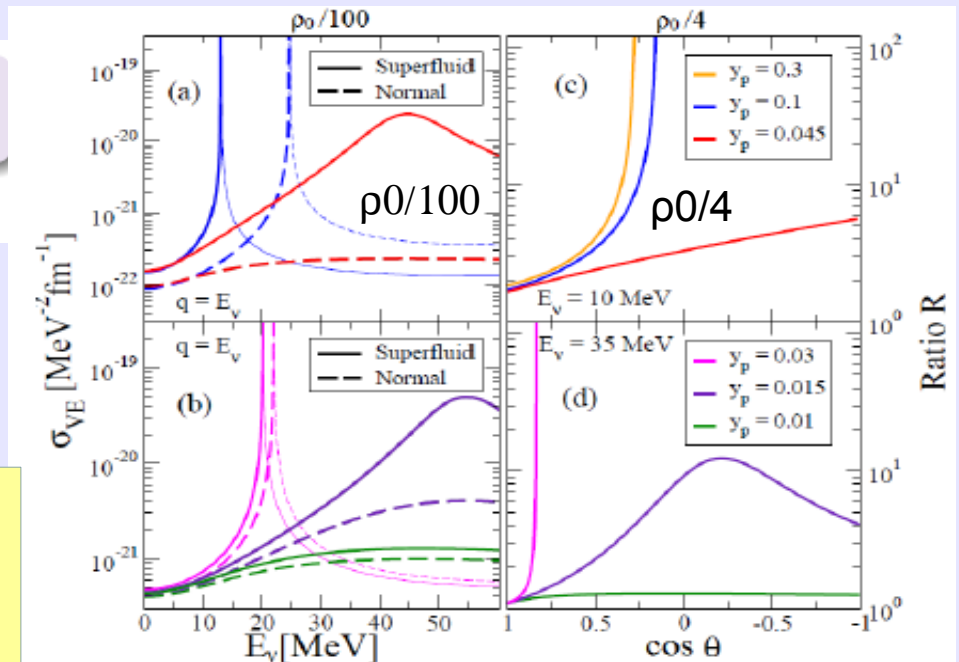
➤ Neutrino transport is influenced by spinodal region

Cooling processes in *supernova explosion and neutron stars*

$$\frac{1}{V} \frac{d^2\sigma}{E_\nu^2 d\Omega^2} = \frac{G_F^2}{4\pi^2} (1 + \cos\theta) T \left[c_V^{(n)^2} C_{nn}^{-1}(q) + c_V^{(p)^2} C_{pp}^{-1}(q) + 2c_V^{(n)} c_V^{(p)} C_{np}^{-1}(q) \right]$$

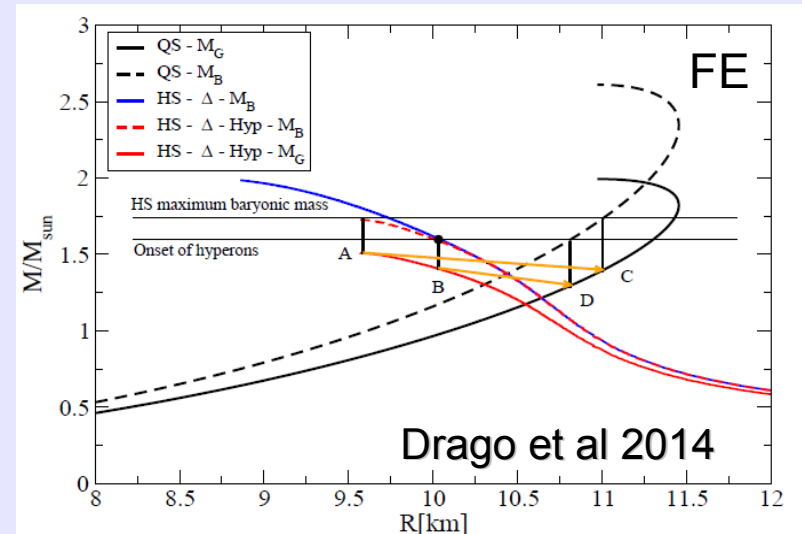
$$c_V^{(n)} = -\frac{1}{2} \quad c_V^{(p)} = \frac{1}{2} - 2\sin^2\theta_W \quad C_{ij}^{-1} \equiv \text{curvature inverse matrix components}$$

At low density and temperature important pairing effects !
 Burrello, Colonna. *Matera*,
 PRC 94, 012801 (2016)

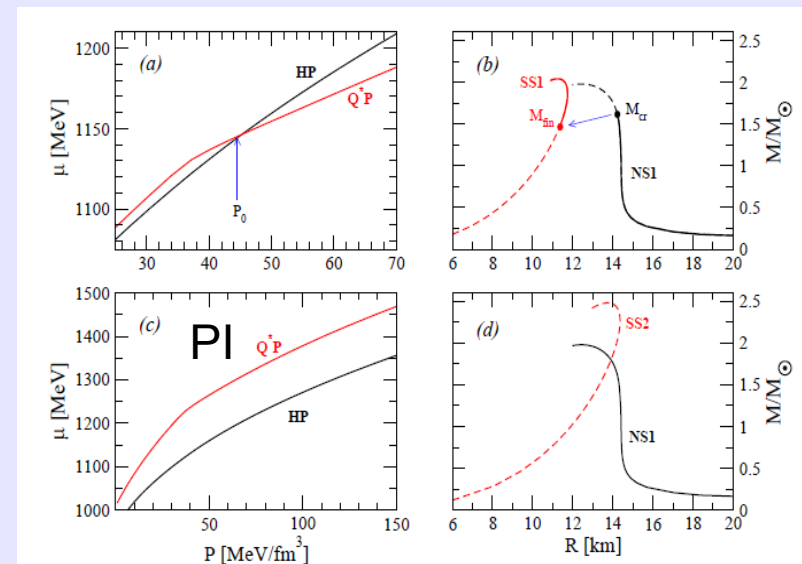


Two families of compact stars?

Main hypothesis: the ground state of nuclear matter is strange quark matter.
 Hadronic stars are metastable and, under some specific conditions, convert into strange quark stars (at fixed baryonic mass the gravitational mass of strange quark stars is smaller).
 Hadronic stars and strange quark stars would populate two separated branches.
 Heavy stars ($2M_{\text{sun}}$) are strange quark stars.



How strong is the softening due to the appearance of heavy baryons on the EoS ?
 How small the radius of hadronic stars? Need of measurements (NICER).



Bhattacharyya et al 2017

Two families of compact stars?

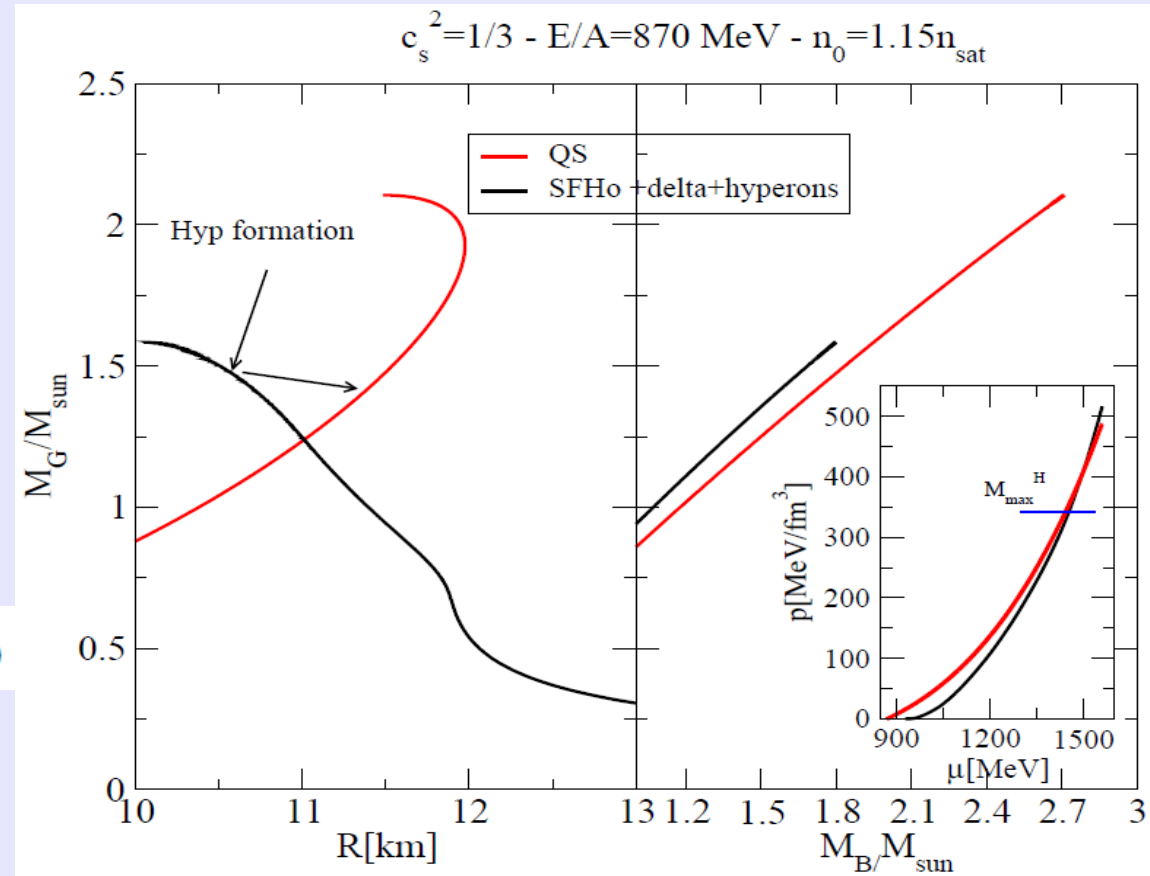
(exercise with constant speed of sound quark EoS, Dondi et al 2016)

Three parameters:
Speed of sound, energy
density and baryon
density at pressure=0

$$p = c_s^2(e - e_0)$$

$$k = \frac{e_0 c_s^2}{1 + c_s^2}$$

$$p = k((n/n_0)^{1+c_s^2} - 1)$$



Hadronic stars would fulfill the small radii limits while strange stars would fulfill the large masses limits. Note: at fixed baryon mass, strange stars could be energetically convenient even if the radius is larger than the corresponding hadronic star configuration.

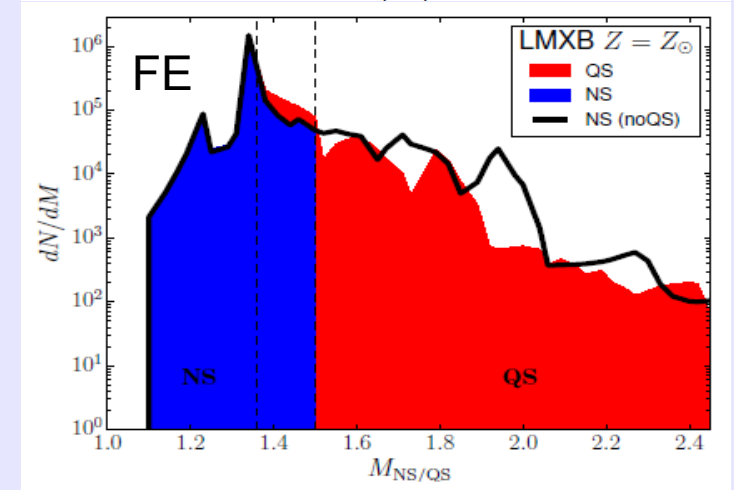
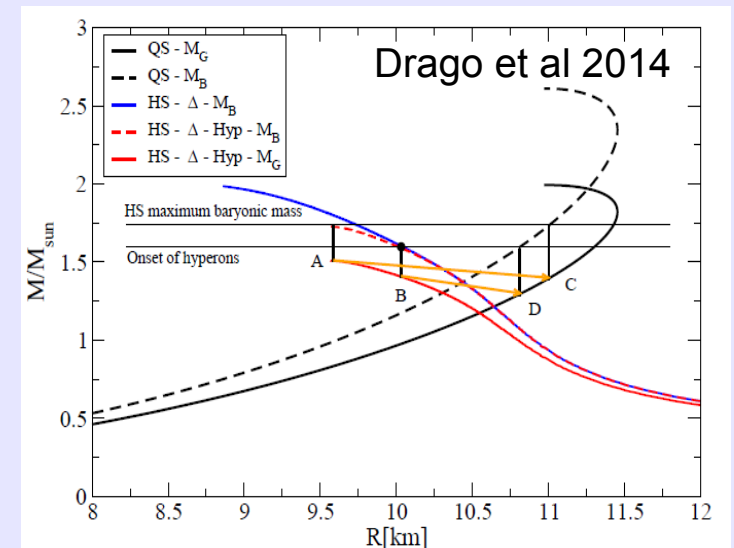
Strange star mergers from population synthesis

(Wiktorowicz et al 2017)
StarTrack code by Belczynski 2002

Simulation of 2 millions binaries with three different metallicities, statistical distributions of progenitor masses, binary separation, eccentricities and natal kicks.

Two families scenario: maximum mass of hadronic stars $1.5-1.6 M_{\text{sun}}$ Massive stars are strange stars.

A small modification of the mass distribution around $1.4 M_{\text{sun}}$



Evolution of two MS stars leading to a double strange star system.

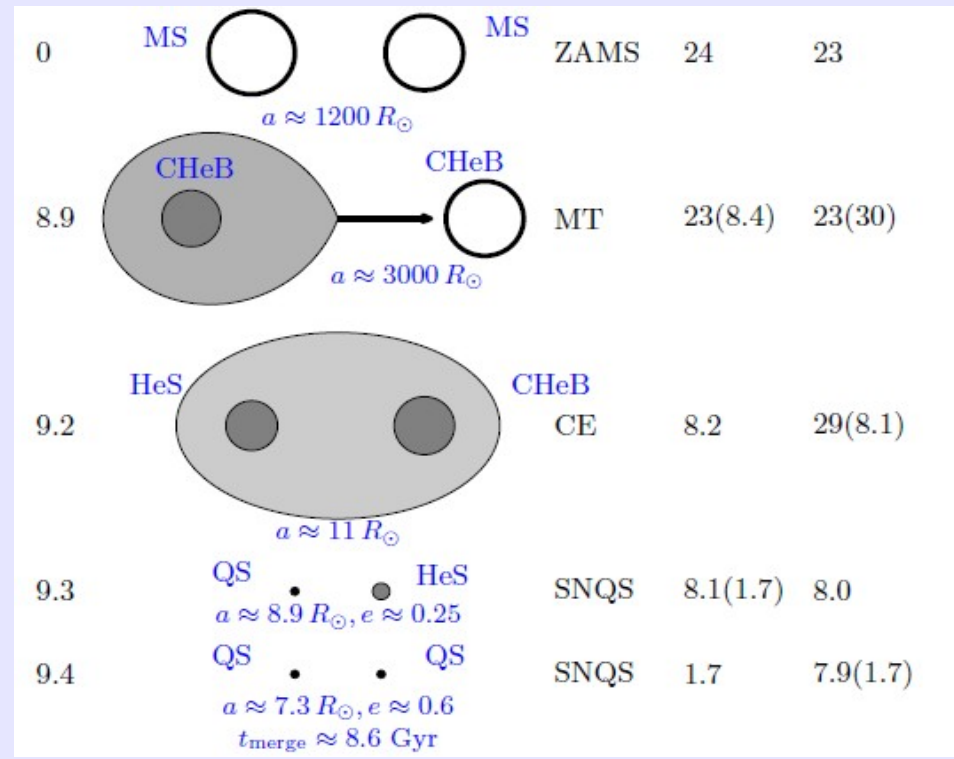


TABLE 1
NUMBER OF QS/NS IN BINARIES

Metallicity	#QS ^a	#NS ^a	f_{QS}^{b}	#NS(noQS) ^c	f_{cr}^{d}
ALL					
Z_{\odot}	9.0×10^4	7.2×10^6	0.01	7.3×10^6	1.10
$Z_{\odot}/10$	2.7×10^5	7.4×10^6	0.04	7.7×10^6	1.37
$Z_{\odot}/100$	1.5×10^5	1.0×10^7	0.01	1.0×10^7	1.57
LMXB					
Z_{\odot}	1.6×10^4	6.1×10^4	0.26	7.7×10^4	1.61
$Z_{\odot}/10$	1.2×10^4	1.5×10^5	0.08	1.6×10^5	1.22
$Z_{\odot}/100$	7.0×10^3	2.1×10^4	0.25	2.9×10^4	1.31
DQS/DNS					
Z_{\odot}	–	6.4×10^5	–	6.6×10^5	0.88
$Z_{\odot}/10$	<u>4.2×10^3</u>	5.2×10^5	0.08	5.2×10^5	1.22
$Z_{\odot}/100$	–	7.6×10^5	–	7.6×10^5	0.86

NOTE. — QS and NS quantities per MWEG at present time for $M_{\text{max}}^{\text{H}} = 1.5 M_{\odot}$. ALL – all binaries; LMXB – mass-transferring binaries; DQS/DNS – double QS/NS.

^a Number of QS (#QS) and NS (#NS)

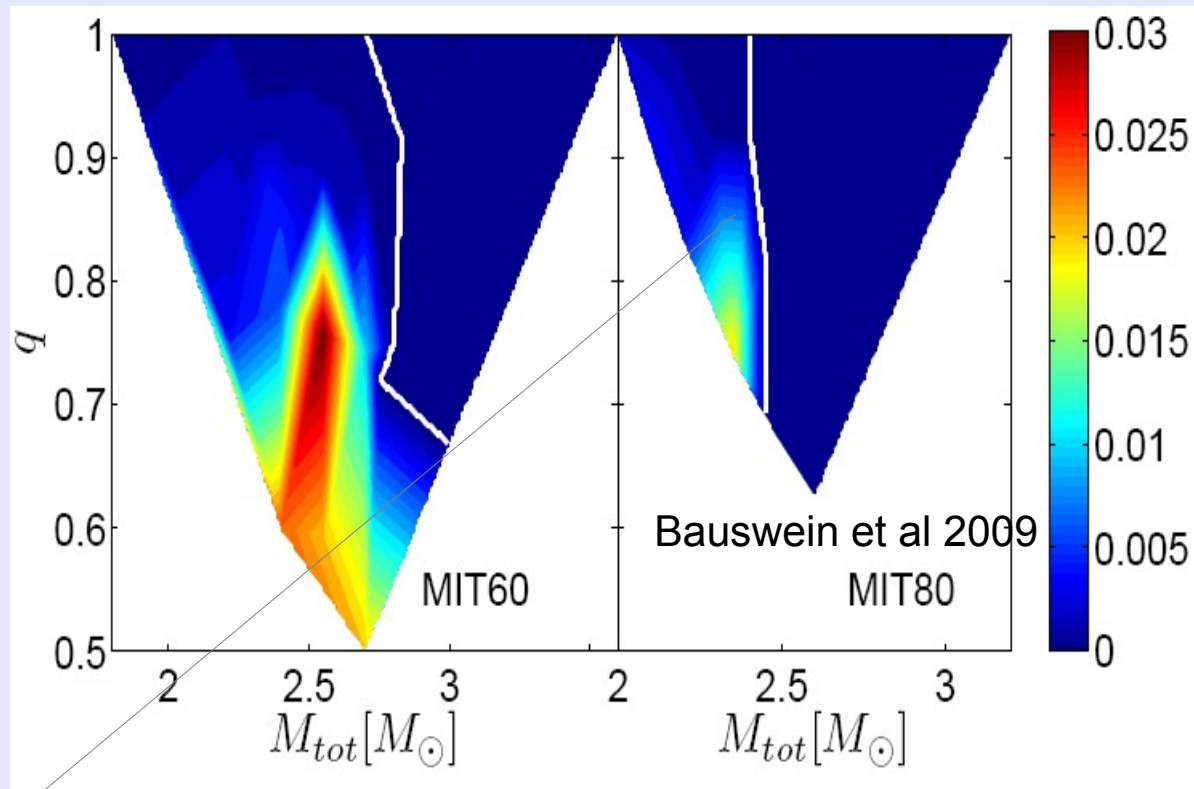
^b fraction of QSs; defined as $f_{\text{QS}} := \#QS / (\#QS + \#NS)$

^c number of NSs in the model without QSs (noQS)

^d change in a number of compact objects (QSs and NSs) in $1.36 - 1.5 M_{\odot}$ mass range; $f_{\text{cr}} := (\#QS' + \#NS') / \#NS'(\text{noQS})$ (mass range marked with ')

**Estimated rate of DQS mergers
(taking into account the
coalescence time): 10/Gyr per
MW galaxy**

Strange quark matter ejecta



Prompt collapse: in those cases no matter ejected (limited by the numerical resolution $10^{-6} M_{\text{sun}}$). In the case of matter ejected, average mass $10^{-4} M_{\text{sun}}$.

To obtain an upper limit: take the typical value of NS mergers, $10^{-2} M_{\text{sun}}$, use the DQS merger rate: strange matter density in the galaxy $\rho_s = 10^{-35-36} \text{ g/cm}^3$.

Flux of strangelets (with a specific value of mass number A , v : velocity of the galactic halo)

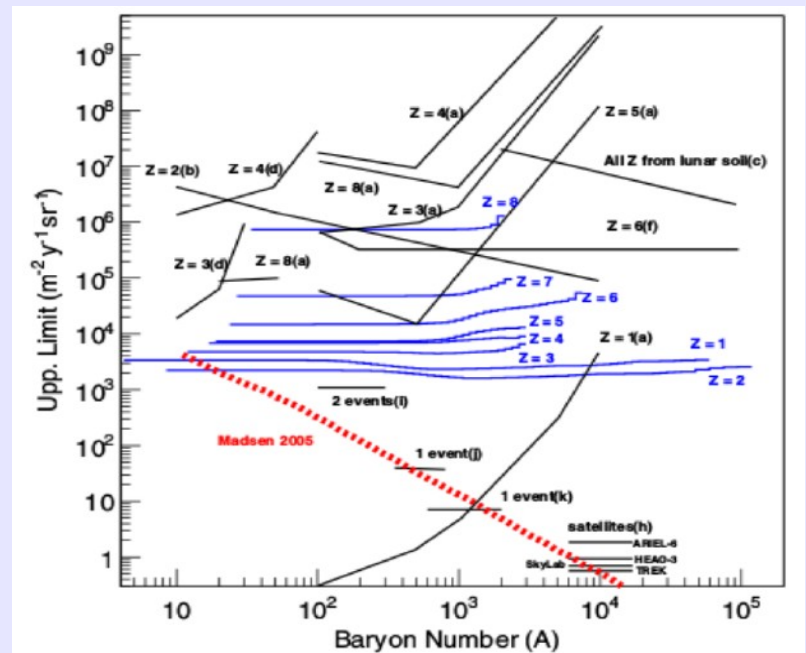
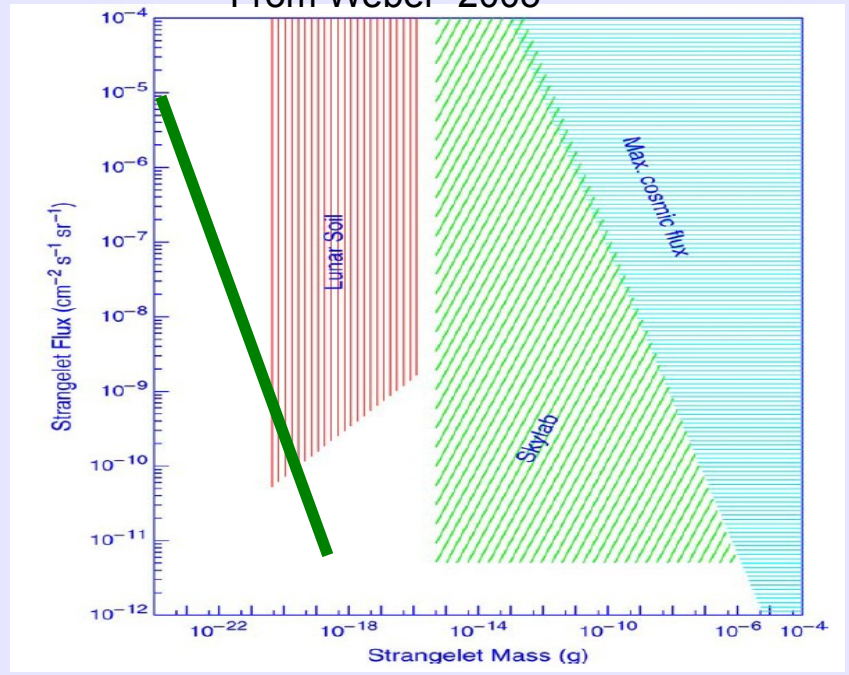
$$\frac{dj_s}{d\Omega} = \frac{\rho_s v}{4\pi A m_p}$$

$$dj_s/d\Omega \sim 10^{-5} \rho_{35}/A \text{ cm}^{-2} \text{ s}^{-1} \text{ sr}^{-1}$$

Considering the extreme upper limit on the mass ejected, our fluxes are compatible with the lunar soil searches.

Constraints from PAMELA: our upper limit violates the limits for $A < 10^3$... but the mass ejected is probably much smaller+difficult to fragment down to such small values of A (work in progress) (PAMELA coll. 2015)

From Weber 2005



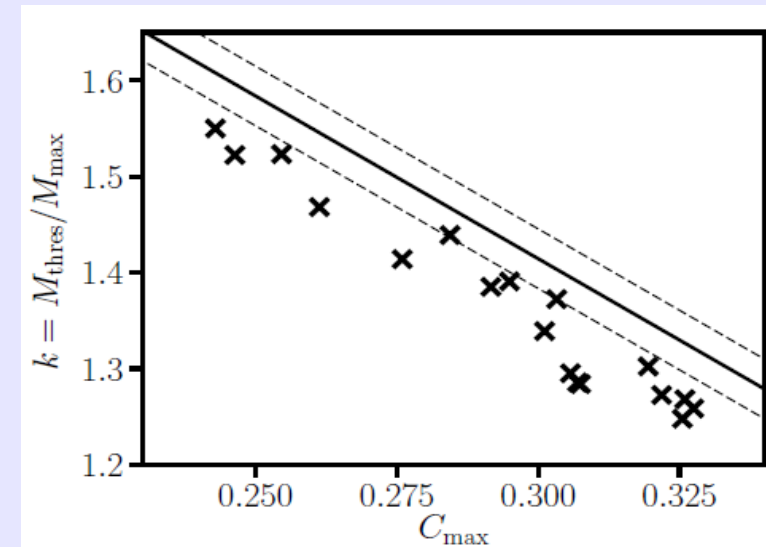
Prediction of the two families scenario on the fate of binary systems

Four possible outcomes (clearly distinguishable from the GWs signals):

- 1) Prompt collapse (large masses)
- 2) Hypermassive (intermediate masses) living ~ 10 ms
- 3) Supramassive stars (living $>$ few sec)
- 4) Stable stars

At fixed total mass, the outcome depends on the EoS. The mass above which a prompt collapse is obtained M_{thresh} is a simple function of M_{max} and its compactness.

Bauswein Stergioulas 2017



Key points of the two families scenario:

1) A merger would always produce at some stage a SS (stable or unstable) but for the case of the prompt collapse

2) In the cases of prompt collapse, the remnant collapses within $t_c \sim \text{few ms}$ which is comparable with the time needed for the turbulent conversion of the hadronic star, t_{turb}

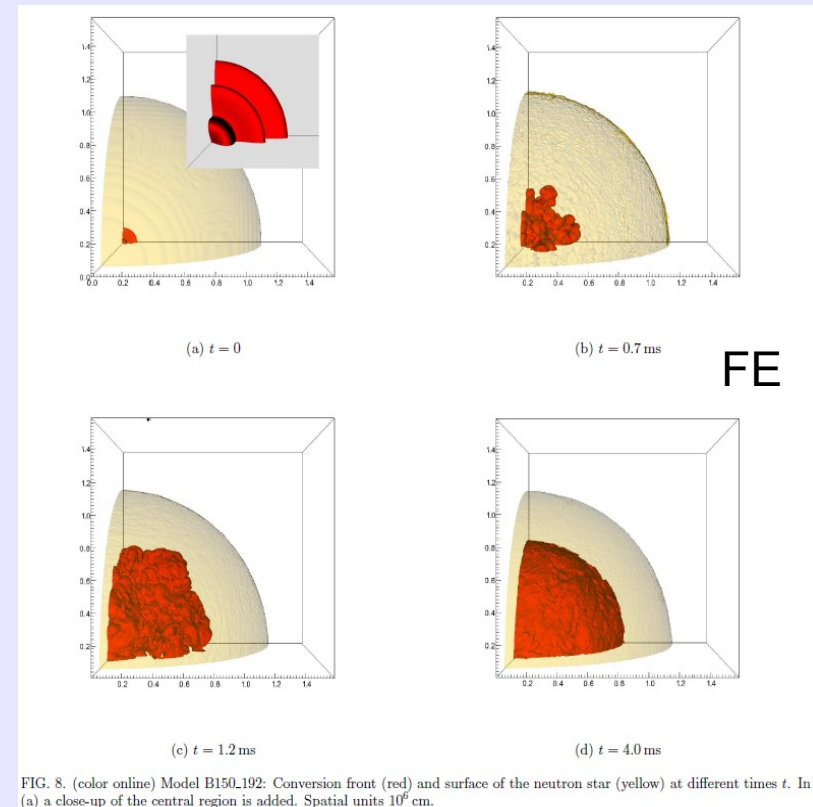
(again few ms, Drago et al 2015)

3) In the cases of prompt collapse the relevant M_{max} is not the maximum mass of SSs but the maximum mass of HSs which is in our scenario of the order of $1.5 - 1.6 M_{\text{sun}}$

We expect therefore to have a large number of cases in which the prompt collapse occurs.

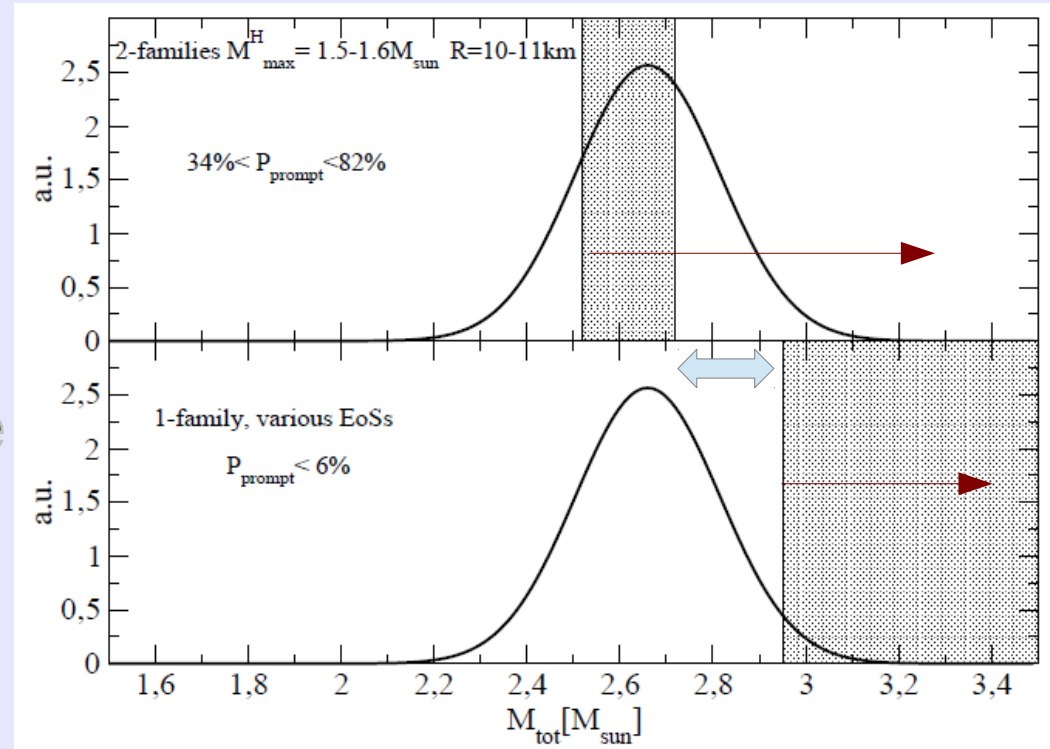
Conversion of a cold, non-rotating hadronic star

(Pagliara et al 2013)



Mass threshold for prompt collapse

By using the binary mass distribution (from Kiziltan 2013) we can calculate the probabilities of prompt collapses in the two families scenario and in the one family scenario.

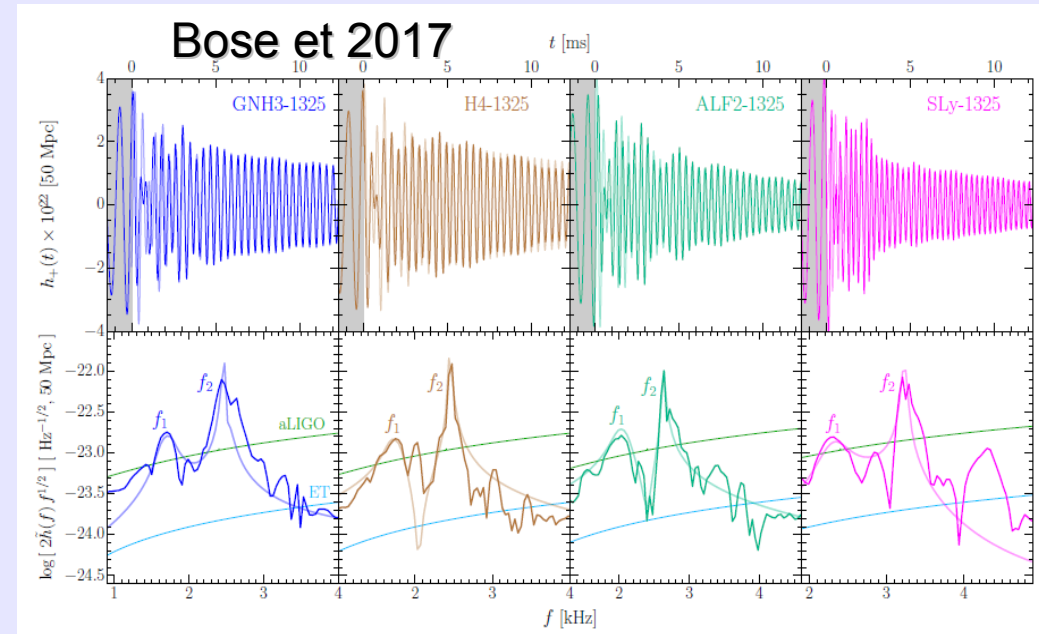


A clear separation of the expected probabilities: a prompt collapse “measured” from direct GW detection

A precise measurement of the total mass could distinguish between the two scenarios even with one (lucky) observation!

Postmerger remnant

If a prompt collapse does not occur, the spectrum of GW shows two clear peaks f_1 and f_2 having a strong correlation with the compactness of the (cold non rotating) star. If the mass is measured, during the inspiral phase, the radius of the cold configuration can be constrained.



Testing the two-families scenario via a direct detection of the fundamental mode of oscillations of the postmerger remnant. High frequency at the beginning of the evolution, clearly different with respect to compact stars within the standard one family scenario.

Stiffening of the equation of state during the conversion and modification on the GW spectrum.

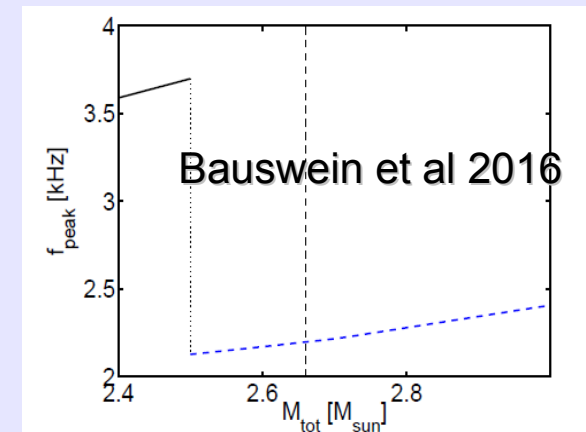


Fig. 17. Dominant postmerger GW frequency f_{peak} as a function of the total binary mass for symmetric mergers with a two-family scenario [46]. For low binary masses the merger remnant is composed of hadronic matter (black curve), whereas higher binary masses lead to the formation of a strange matter remnant with a lower peak frequency (dashed blue curve). The vertical dashed line marks a lower limit on the binary mass which is expected to yield a remnant that is stable against gravitational collapse (see text).

Conclusions

New observations are upcoming, a new tool: gravitational wave astronomy. Possibility to test in the near future the existence of exotic matter in compact stars through radii/compactness measurements:

- NICER direct measurement
- GWs from the postmerger remnant and frequency of the f_{1-2} modes
- Radio measurements of the moment of inertia (if a $R_{1.4}$ turns out to be smaller than about 11km, it would be a strong indication of “exotic matter” in compact stars)

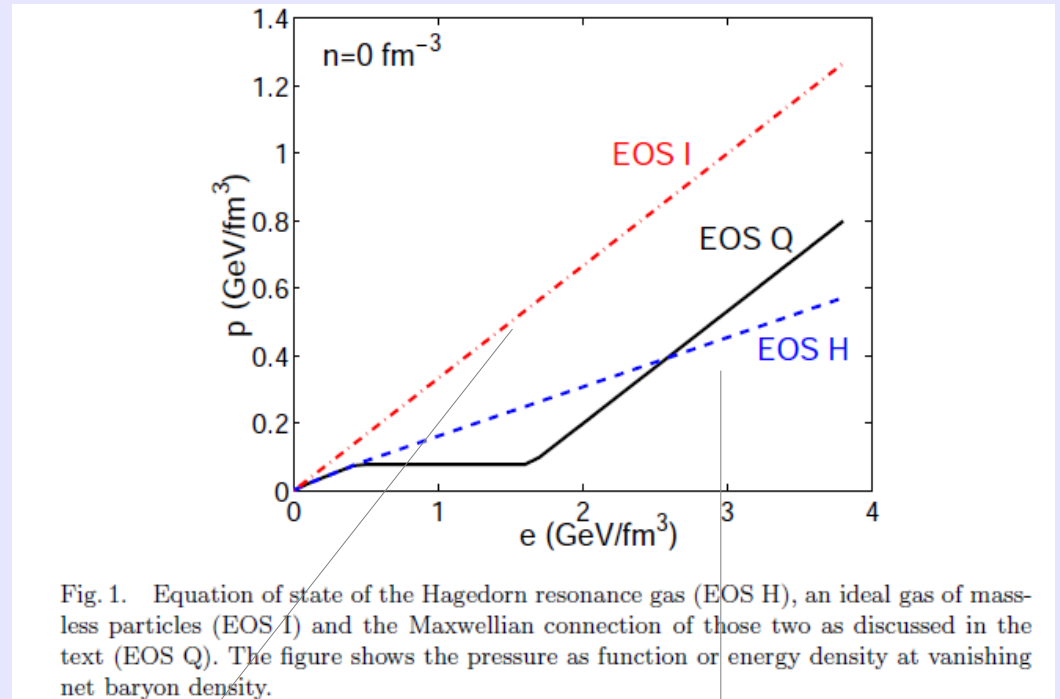
Probing the composition: cooling, glitches (pairing), neutrinos (in case of a galactic SN)

Appendix

... is this surprising?

Heavy ions physics: (Kolb & Heinz 2003)

Also at finite density the quark matter equation of state should be stiffer than the hadronic equation of state in which new particles are produced as the density increases



$p=e/3$ massless quarks

Hadron resonance gas
 $p=e/6$

Fragmentation

Work in progress

Condition to create a fragment: Weber number We larger than 1

$We = (\rho/\sigma) v_{\text{turb}}^2 d$ (mass density, surface tension, turbulent velocity and drop size). By assuming v_{turb}^2 to scale (Kolmogorov) with $v_0^2 (d/d_0)^{5/3}$ where $d_0 \sim 1\text{km}$ and $v_0 \sim 0.1c$, we obtain $d \sim 1\text{mm}$ and thus $A \sim 10^{39}$ **very big fragments**. There will be a further “reprocessing” via collisions, turbulence, evaporation ... very difficult problem!!
There will be a distribution of mass number, with a minimum value which is probably much higher than 10^3 .

Depending on the size, different strangelets can act as seeds for the conversion of stars into strange stars (astrophysical argument againsts the Witten's hyp.).

Capture of strangelets by stars and conversion

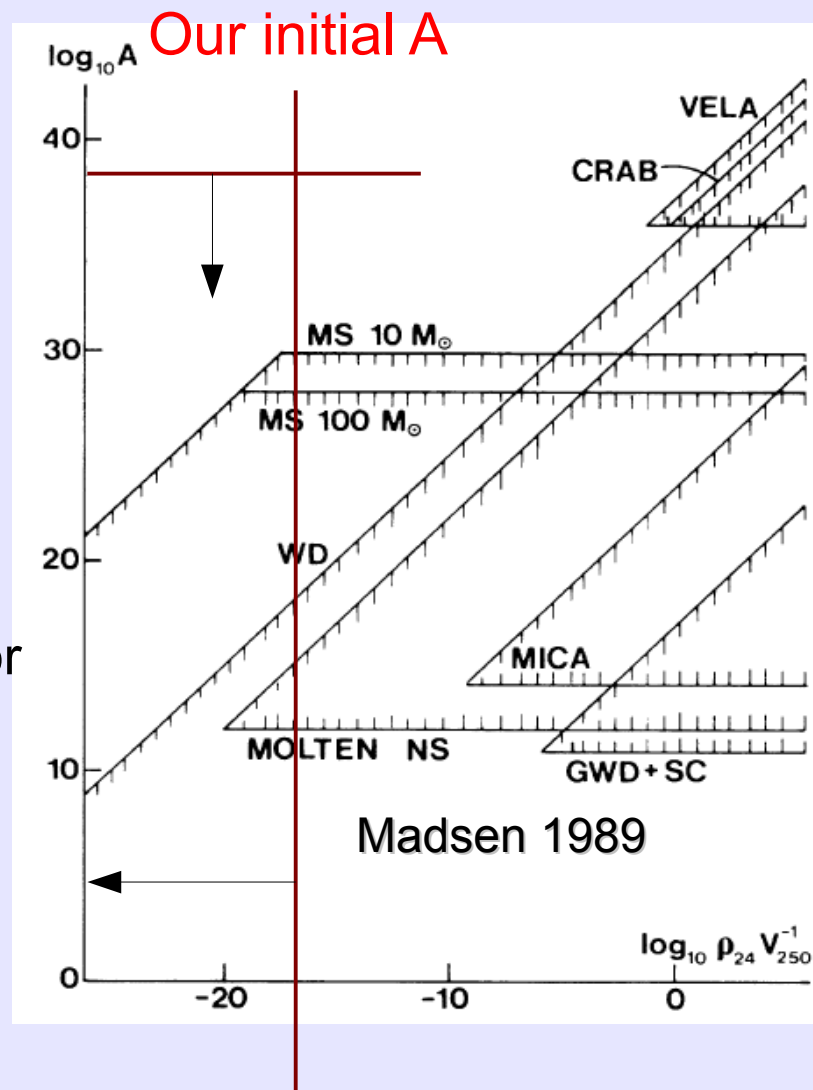
$$mv(x) \frac{dv(x)}{dx} = -\alpha \rho(x) v^2(x) + \frac{GM(x)m}{R^2(x)} - \epsilon(x)\alpha$$

Stopping force due elastic interaction with atoms

Interaction with the ion lattice

Main sequence stars: the most important limit. A strangelet can sit in the center of the star and “wait” for the core collapse SN and the neutronization. This would trigger the conversion of all protoneutron stars into strange stars.

- But:**
- 1) due to the 10 MeV temperature of the SN they could evaporate
 - 2) Not clear if fragmentation can work over ten orders of magnitude. Work in progress.



Our upper limit on the strange matter density

A recent intriguing observation (needs more statistics)

Muon Bundles as a Sign of Strangelets from the Universe

P. Kankiewicz¹, M. Rybczyński¹, Z. Włodarczyk¹, and G. Wilk²

¹Institute of Physics, Jan Kochanowski University, 25-406 Kielce, Poland; pawel.kankiewicz@ujk.edu.pl,
maciej.rybczynski@ujk.edu.pl, zbigniew.wlodarczyk@ujk.edu.pl

²National Centre for Nuclear Research, Department of Fundamental Research, 00-681 Warsaw, Poland; grzegorz.wilk@ncbj.gov.pl

Received 2016 December 30; revised 2017 March 17; accepted 2017 March 17; published 2017 April 11

Abstract

Recently, the CERN ALICE experiment observed muon bundles of very high multiplicities in its dedicated cosmic ray (CR) run, thereby confirming similar findings from the LEP era at CERN (in the CosmoLEP project). Originally, it was argued that they apparently stem from the primary CRs with a heavy masses. We propose an alternative possibility arguing that muonic bundles of highest multiplicity are produced by strangelets, hypothetical stable lumps of strange quark matter infiltrating our universe. We also address the possibility of additionally deducing their directionality which could be of astrophysical interest. Significant evidence for anisotropy of arrival directions of the observed high-multiplicity muonic bundles is found. Estimated directionality suggests their possible extragalactic provenance.

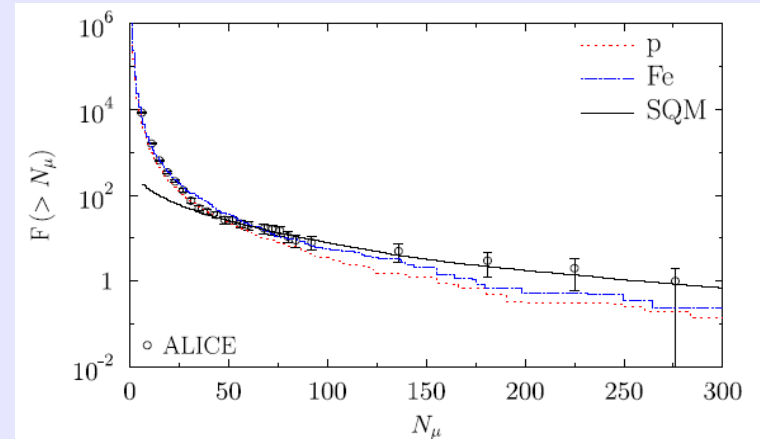


Figure 4. Integral multiplicity distribution of muons for the ALICE data (The ALICE Collaboration 2016b) (circles). Monte Carlo simulations for primary protons (dotted line); iron nuclei (dashed dot line) and primary strangelets with mass A taken from the $A^{-7.5}$ distribution (full line) with abundance (at $A = A_{\text{crit}}$) $2 \cdot 10^{-5}$ of the total primary flux.

If true it would imply that also MS stars have captured strangelets